

Full Recovery of Electron Damage in Glass at Ambient Temperatures

K. A. Mkhoyan,¹ J. Silcox,¹ A. Ellison,² D. Ast,³ and R. Dieckmann³

¹*School of Applied and Engineering Physics, Cornell University, Ithaca, New York 14853, USA*

²*Corning Incorporated, Corning, New York 14831, USA*

³*Department of Material Science and Engineering, Cornell University, Ithaca, New York 14853, USA*

(Received 23 November 2005; published 26 May 2006)

An unusually complete recovery of extensive electron-beam-induced damage in a thin film of a CaO-Al₂O₃-SiO₂ glass was discovered. Nanoscale measurements show that the Ca ions migrate about 10 nm away during irradiation and return during recovery. Oxygen atoms are trapped largely as molecular oxygen and do not migrate. Electron energy loss measurements demonstrate that the glass returns completely to the original compositional and structural state thus indicating that the glass is in a deep thermodynamic energy minimum.

DOI: [10.1103/PhysRevLett.96.205506](https://doi.org/10.1103/PhysRevLett.96.205506)

PACS numbers: 61.43.Fs, 61.80.Fe, 61.82.Rx, 68.37.Lp

In this Letter, we report nanoscale measurements of the chemical changes observed in an apparently complete reversal of electron damage in a silicate-based glass system at ambient temperature. This phenomenon is rarely found but these observations offer interesting insights into the underlying mechanisms. Silicate-based glass can be readily damaged by ion beams [1,2], electron beams [3,4], or UV beams [5,6]. The damage is normally considered irreversible and is sometimes used to deliberately modify the initial network [7,8]. The conditions under which recovery may happen are identified here and suggest a method to search for additional systems. Since the damaged system reverts to a condition identical with the initial condition, we conclude that the initial thermodynamic state of the glass is a very deep energy minimum and is very stable. The observations suggest that nonglass forming elements are able to move surprisingly long distances (~ 10 nm) in the glass at room temperature under the influence of a high electrostatic field and that the recovery level depends on the way in which the glass handles excess oxygen. Whether these observations have any impact on the long term encapsulation of radioactive materials remains to be seen.

The experiments were carried out in a Vacuum Generator HB-501 100 kV scanning transmission electron microscope (STEM) that produces a focused electron probe of ~ 2.1 Å in diameter with a beam current of ~ 15 pA and is equipped with a cold field emission gun, a single-electron sensitive annular dark field (ADF) detector, and a parallel electron energy loss spectrometer (EELS) [9]. Compositional changes can be measured on a spatial scale as small as the atomic scale [9,10]. To create electron-beam-induced damage in the glass of composition (CaO-Al₂O₃)_{0.9}(2SiO₂)_{0.1} [11], the scanning electron probe in STEM was concentrated on a small square area of 6.3×6.3 nm² with a beam current density of ~ 40 A/cm² [12]. The thicknesses of the areas of the glass used in measurements were estimated using low-loss EELS [14] and were around 300 Å. During exposure of the area the changes in the chemical composition of the glass were

studied by simultaneously recording ADF images and core-level EELS spectra of the components: O *K* edge with 10 sec of acquisition time, Ca *L*_{2,3} (with 6 sec), and Al *L*_{2,3} and Si *L*_{2,3} edges (with 2 sec). After intentionally damaging the glass for a short period of time, the beam was deflected away from the damaged area. The recovery process was studied by periodically recording ADF images of the damaged area. When the glass was recovered, the EELS spectra of the same components from exactly the same area were measured again.

Composition sensitive ADF images taken before and after damage and during recovery are presented in Figs. 1(a)–1(d). Here 2 min of extensive electron-beam-induced damage was applied to a small area and then recovery was monitored at 30 sec intervals. It took only 2 min for sample to fully recover. Figure 1(e) shows the profiles of the line scans of the same damaged area obtained from images 1(a)–1(d). The intensity of the ADF signal drops dramatically indicating heavy mass loss in the damaged area. The intensity difference between the line scans in (a) and (b) is presented in Fig. 1(f). The increase in the ADF intensity in the region immediately surrounding the damaged area indicates mass accumulation in that area. The total ADF signal calculated by integrating the intensities of the images (a) and (b), recorded before and after damage, proved to be the same suggesting that there has been no loss of total mass. Since ADF imaging gives only the changes in the mass distribution, possible structural and compositional changes (e.g., phase transitions, etc.) require core-level EELS analysis.

Figure 2 shows changes in the EELS spectra of the Ca *L*_{2,3} and O *K* edges with progressive damage [15]. A significant reduction of the intensity of the Ca *L*_{2,3} edge occurred but no visible changes in the fine structure was observed. In contrast, the fine structure of the O *K* edge undergoes dramatic changes with damage. A new peak appears at ~ 531 eV indicating that a significant amount of molecular oxygen (O₂) [4,16,17] is formed in the damaged area. The EELS spectra recorded after recovery show

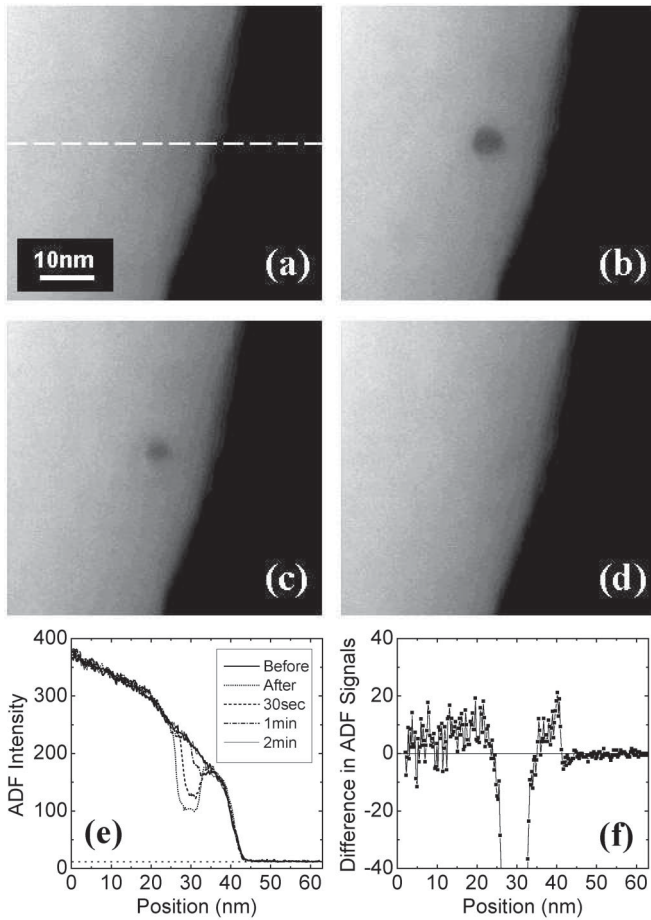


FIG. 1. ADF images of glass particle. (a) Before the damage, (b) after 2 min of electron-beam damage (only $6.3 \times 6.3 \text{ nm}^2$ area was damaged); (c)–(d) images recorded after 30 sec and 2 min of recovery with beam turned off; (e) line scans of the ADF intensities across damaged area [dashed line in (a)] obtained from images before and after damage [images (a) and (b)] and during recovery; (f) difference between line scans from (b) and (a).

that the fine structure as well as the intensities of the Ca $L_{2,3}$ and O K edges are fully restored. Since the recording time of each spectrum is of the order of several seconds, their acquisition is always accompanied with damage of the glass. Thus, as in Fig. 2(b), both the initial and the final (after recovery) spectra contain signals of molecular O_2 .

For quantitative analysis the integrated intensities of the Ca $L_{2,3}$ and O K edges were calculated and are presented in Fig. 3. Here the data were normalized to the undamaged state. In parallel with the ADF intensity data, a decline in the intensity of the Ca $L_{2,3}$ edge with continuous damage is measured; about 35% of the total Ca is removed within the first 2 min. The total intensity of the O K edges, however, as can be seen in Fig. 3(a), does not change at all suggesting that the number of oxygen atoms in the damaged area of glass stays constant. The amount of created O_2 was calculated by fitting the measured peak at 531 eV to the

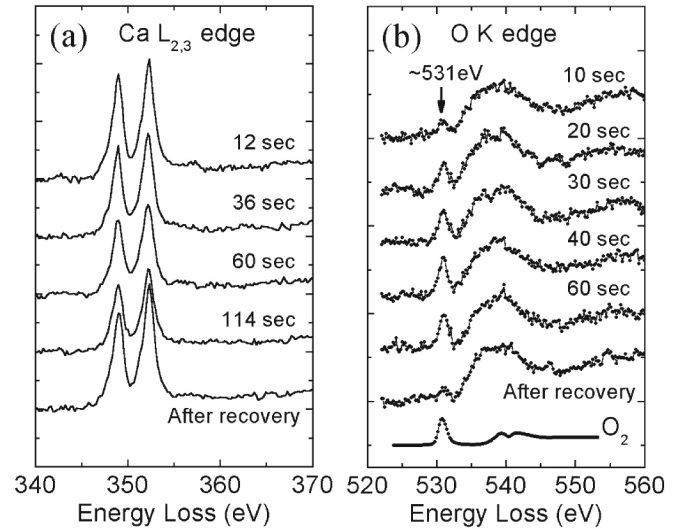


FIG. 2. (a) Evolution of the spectra of Ca $L_{2,3}$ edge and (b) O K edge with continues damage. The bottom spectra in (a) and (b) were recorded after recovery, having beam off for 2 min. Spectrum of the O K edge of O_2 is reproduced from Ref. [16].

corresponding O_2 peak and calculating the ratio of the integrated intensities of the O K edges in O_2 and the total. The results show that about 33% of the total oxygen in the glass is transformed into molecular O_2 [see Fig. 3(b)]. From the stoichiometry of this glass only 22.5% of the oxygen is bound to Ca, suggesting that it is not just oxygen atoms freed from the Ca-O bonds that are transformed into O_2 . At least 14.6% of O_2 must be generated by breaking

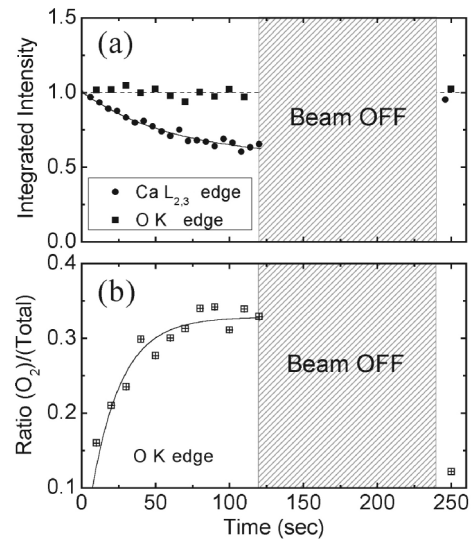


FIG. 3. (a) Changes in integrated intensity of the Ca $L_{2,3}$ edge calculated using 346 to 354 eV energy range and the O K edges, calculated using 525 to 555 eV energy range, with electron-beam exposure; (b) the ratio of the integrated intensity of the O K edge in O_2 to the total intensity of O K edge. The decay of Ca $L_{2,3}$ edge is proportional to $\exp[-t/62]$, whereas the increase of the ratio $(\text{O}_2)/(\text{total})$ is proportional to $\exp[-t/20]$.

Al-O and Si-O bonds. This conclusion is also apparent from the rates of reduction of Ca $L_{2,3}$ edge and the increase in the O_2 /(total oxygen) ratio. Exponential fits (see Fig. 3) show that the increase of the O_2 /(total oxygen) ratio is about $3\times$ faster than the reduction of the Ca. Observations of the O_2 created due to electron-beam damage in amorphous and crystalline Al_2O_3 have been reported by Humphreys and co-authors [18]. Stevens-Kalceff [19] reported that O_2 can also be formed radiolytically in amorphous and crystalline SiO_2 when irradiated by electron beam. Finally, we conclude that since there is no oxygen-loss, the O_2 must remain trapped in the sample.

The results summarized in the previous two paragraphs establish that there is no mass loss during irradiation; the calcium migrates to the periphery of the irradiated area while the oxygen remains within that area although the bonding state changes significantly. Zero mass loss is a necessary condition for complete damage recovery. Clearly, the molecular oxygen is trapped in the structure. Then, since some of the molecular oxygen must be formed from the glass forming units (Al_2O_3 , SiO_2), there should be modifications in the network itself resulting from damage. Figure 4(a) shows the recorded EELS spectra of the Al $L_{2,3}$ edge measured from this glass and also, for comparison, from amorphous Al_2O_3 . All the major features are labeled A to F. The unusually weak Si signal—three small bumps labeled G, H, and I—is the result of the extremely low concentration of SiO_2 in this glass. Comparison of these two spectra shows that $L_{2,3}$ edge measured in the undamaged glass has more and better defined peaks (B-E) than in $a-Al_2O_3$. Briefly put, disordered solids exhibit very little fine structure in EELS spectra whereas solids with

crystalline order exhibit sharp features in the fine structure of the core edges [for details see Section 5.6 of Ref. [14]]. We can, therefore, argue that the coordination number of the Al atoms in the undamaged glass is higher than in $a-Al_2O_3$ suggesting order, perhaps paracrystallinity, of the glass network. Bouchet and Colliex [20] report that the higher the coordination of the Al in different Al_2O_3 compositions the finer is the structure of the $L_{2,3}$ edge spectrum (with a bigger number of peaks). In damaged glass, as can be seen from Fig. 4(b), the Al spectrum is close to that of $a-Al_2O_3$.

After recovery, the system returns to the original state, both compositionally (Fig. 3) and, probably, structurally [Fig. 4(b)]. The dynamic physical picture is the following: as in most insulators in the glass the electron beam irradiated area is positively charged due to the emission of secondary electrons from the area. When dynamic equilibrium is reached, this charge is partially compensated by the influx of conducting electrons from neighboring areas [21]. At the same time breakage of Ca-O bonds (~ 2 eV) occurs due to ionization of the nonbridging oxygen bonds [4]. The positive charge created in the network will be mostly trapped at dangling bonds. The resulting large electric field [~ 10 kV/cm [21,22]] caused by total positive charge drives the free Ca ions from the region, as we observed in Figs. 2 and 3. These positive Ca ions drift ~ 10 – 15 nm (see Fig. 1) into the peripheral undamaged region prior to neutralization. The free oxygen atoms combine creating molecular oxygen. When irradiation is stopped, the positive charge of the network will be fully compensated by electron flow; the Ca atoms will diffuse back and recombine with the trapped oxygen atoms. At this stage, however, it is not clear what driving forces actually control the diffusion of these Ca atoms.

To understand why recovery of electron-beam-induced damage created under similar irradiation doses has not been observed previously [3,4], another set of identical experiments on a different glass $(CaO-Al_2O_3)_{0.67}-(2SiO_2)_{0.33}$ with a higher silica fraction was conducted. The results showed that the processes occurring during the damage: expulsion of Ca from the area, formation of O_2 , constancy of total amount of oxygen, etc., are similar to those in the first glass. However, the recovery is significantly different. This glass recovers only partially. ADF signals indicate only $\sim 90\%$ mass recovery and O K edge recorded after partial recovery still contain $\sim 20\%$ of molecular O_2 [13].

The damage process creates dangling bonds in the glass network in addition to the changes outlined above. Studies on amorphous SiO_2 shows that O_2 produced during damage can bond to the silicon dangling bonds [E' centers [23]] forming peroxy radicals and links [24–27]. It seems that the effect of the increased silica fraction in the second glass is to increase the number of oxygen atoms locked into defect bonding configurations in the network, thereby re-

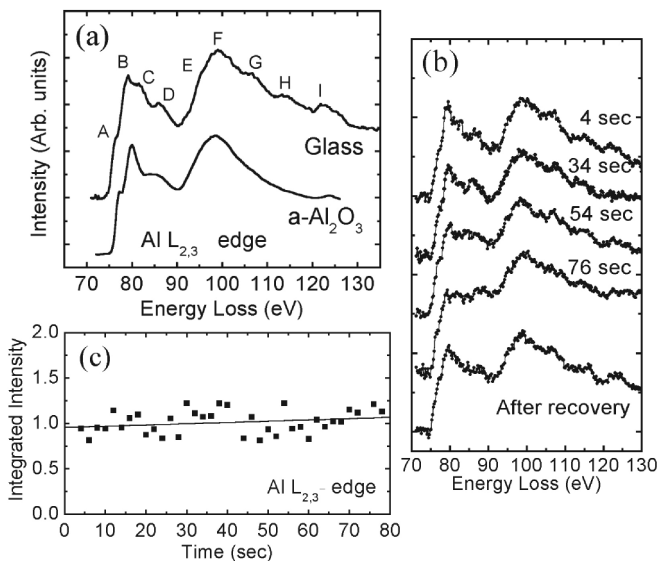


FIG. 4. (a) Measured EELS spectra of the Al and Si $L_{2,3}$ edges; (b) evolution of this spectra with continues damage and the recovery after 2 min. (c) Integrated intensity (from 74 to 90 eV energy range) of the Al $L_{2,3}$ edge with continues damage.

ducing the number of possible nonbridging sites for reabsorption of the calcium.

The conditions under which recovery of this type can occur are summarized in the following. First, no mass loss should occur. In thin film specimens, eventual removal of atoms is almost inevitable unless the bonding is extremely strong. Thus the irradiation time should be less than the time necessary for significant mass loss to occur. Second, diffusion must be sufficient at the ambient temperature for atoms to migrate back to suitable bonding sites. In the present case, the displacement of ~ 10 nm in a time ~ 100 sec suggests a diffusion coefficient of 10^{-14} cm²/sec. Third, the role of oxygen is critical: unless the oxygen is available for recombination with the displaced atoms then recovery is incomplete. Trapping of oxygen into defect bonding configurations in the network may be a factor in the incomplete recovery of the high-SiO₂-composition glasses. An additional observation is that surface diffusion seems not to be an issue in this situation. Since there is no mass loss within our experimental limits, it seems clear that surface diffusion does not play a major role in these experiments since the molecular oxygen would clearly leave the system. Finally, the observation that the system recovers so completely (structurally, as well as compositionally) after such a substantial perturbation is evidence that the initial state of the glass must be a very stable thermodynamic minimum.

This work is supported primarily by the Nanoscale Science and Engineering Initiative of the NSF EEC-0117770 and NYSTAR C020071. The sample preparation facilities and STEM are supported by NSF through the Cornell Center of Materials Research DMR 9632275.

-
- [1] T. W. Hickmott, Phys. Rev. Lett. **32**, 65 (1974).
 [2] E. Valentin, H. Bernas, C. Ricolleau, and F. Creuzet, Phys. Rev. Lett. **86**, 99 (2001).
 [3] N. Jiang and J. Silcox, J. Appl. Phys. **92**, 2310 (2002).
 [4] N. Jiang, J. Qiu, A. Ellison, and J. Silcox, Phys. Rev. B **68**, 064207 (2003).
 [5] K. Kajihara, L. Skuja, M. Hirano, and H. Hosono, Phys. Rev. Lett. **89**, 135507 (2002).
 [6] Y. Shimotsuma, P. G. Kazansky, J. Qiu, and K. Hirao, Phys. Rev. Lett. **91**, 247405 (2003).
 [7] N. Chiodini, A. Paleari, and G. Spinolo, Phys. Rev. Lett. **90**, 055507 (2003).
 [8] D. Rugar, R. Badakian, H. J. Mamin, and B. W. Chui, Nature (London) **430**, 329 (2004).
 [9] K. A. Mkhoyan, E. J. Kirkland, J. Silcox, and E. S. Allredge, J. Appl. Phys. **96**, 738 (2004).
 [10] D. A. Muller, T. Sorsch, S. Moccio, F. H. Baumann, K. Evans-Lutterodt, and G. Timp, Nature (London) **399**, 758 (1999).
 [11] Specimens for electron microscopy were prepared by grinding small quantities of glass into a powder in isopropanol and mounting suspended pieces on a thin holey-carbon-film covering a copper grid. This method provides specimens with a variety of sizes and prevents surface contamination.
 [12] Temperature increase in the exposure area was estimated using Bethe expression for mean energy loss per unit path of incident electron. For the conditions of conducted experiments, in irradiated area, temperature is expected to rise not more than few degrees (< 5 °C) [13].
 [13] K. A. Mkhoyan and J. Silcox, (unpublished work).
 [14] R. Egerton, *Electron Energy Loss Spectroscopy in the Electron Microscope* (Plenum, New York, 1996).
 [15] In all core-level EELS data presented here the backgrounds were subtracted using conventional $f(E) = AE'$ fitting function.
 [16] Y. Ma, C. T. Chen, G. Meigs, K. Randall, and F. Sette, Phys. Rev. A **44**, 1848 (1991).
 [17] A. P. Hitchcock and C. E. Brion, J. Electron Spectrosc. Relat. Phenom. **18**, 1 (1980).
 [18] S. D. Berger, I. G. Salisbury, R. H. Milne, D. Imeson, and C. J. Humphreys, Philos. Mag. B **55**, 341 (1987); C. J. Humphreys *et al.*, Scanning Microsc. **4**, 185 (1990).
 [19] M. A. Stevens-Kalceff, Phys. Rev. Lett. **84**, 3137 (2000).
 [20] D. Bouchet and C. Colliex, Ultramicroscopy **96**, 139 (2003).
 [21] L. W. Hobbs, in *Introduction to Analytical Electron Microscopy*, edited by J. J. Hren *et al.* (Plenum, New York, 1979), p. 437.
 [22] J. Cazaux, Ultramicroscopy **60**, 411 (1995).
 [23] D. L. Griscom, E. J. Friebele, and G. H. Sigel, Solid State Commun. **15**, 479 (1974); D. L. Griscom, Phys. Rev. B **20**, 1823 (1979).
 [24] E. J. Friebele, D. L. Griscom, M. Stapelbroek, and R. A. Weeks, Phys. Rev. Lett. **42**, 1346 (1979).
 [25] D. L. Griscom and E. J. Friebele, Phys. Rev. B **24**, R4896 (1981).
 [26] R. L. Pfeffer, in *The Physics and Technology of Amorphous SiO₂*, edited by R. A. B. Devine (Plenum, New York, 1988), p. 181.
 [27] T. E. Tsai and D. L. Griscom, Phys. Rev. Lett. **67**, 2517 (1991).